https://doi.org/10.2352/ISSN.2169-2629.2018.26.396

Color Management in 3D Fine-Art Painting Reproduction

M. K. Jackson; Arius Technology Inc.; Vancouver, Canada and L. W. MacDonald; MacColour Ltd.; Stratford-upon-Avon, UK.

Abstract

We propose and discuss a color-managed workflow for 3D fine-art imaging based on a lookup-table-based transformation to match colors from a laser-scanned 3D image to those from a photographic reference image. We show the significant color errors from shaded, shadowed and specular pixels in the reference image can be eliminated using geometric information from the laser scans.

Introduction

Color scanning presents a rich source of information for fine art painting conservation. A famous 2004 study by a team of imaging scientists from the National Research Council of Canada used high-resolution three-dimensional (3D) scanning of the *Mona Lisa* to study its structure and the sfumato painting technique used by Leonardo [1]. Advances in 3D color printing now enable reproduction of the color and geometry of masterworks of art with unprecedented fidelity. This new reprographic technology poses unique challenges that are not addressed by the color management techniques that have served the graphic arts industry to date. The root cause of the new challenges is that the manifestation of photometric effects occurs at a different point in the reproduction workflow. In the traditional graphic arts, real objects are illuminated with one or more light sources and then photographed. Capturing the image fixes (or "bakes in") all the photometric aspects of the scene at the instant of capture, including specular highlights, cast shadows and shading caused by the orientation of the object surface relative to the illumination source(s) and the camera's point of view. The goal is to achieve in print a faithful reproduction of the image observed by the camera, complete with all the photometric details visible at the point and instant of capture.

3D reprographics has at its core a key difference. When a real item is digitized, then printed in 3D, the geometry and surface color should be a facsimile of the shape and color of the original object, not of its appearance. Then the resulting object will faithfully reproduce the appearance of the original object when illuminated with similar light sources and viewed from similar positions. Ideally the spectral reflectance of the 3D print should be identical at every point to that the original, but because of metamerism of the colorants this is generally not possible. At least it should be an exact color reproduction, in Hunt's terminology [2].

It is therefore essential that the color of the original be encoded in a way that is independent of all aspects relating to the illumination used during capture: luminance non-uniformity, specular highlights, cast shadows and shading must be removed. Then when the 3D reproduction is illuminated, it will by its shape, surface color and gloss recreate the same photometric effects present when viewing the original. It is acceptable in 2D reproductions for the flat print to contain highlights representing the appearance of specular highlights. However, in a 3D reproduction it is essential for such highlights to be absent from the color so that the physical object itself may recreate them, from whatever viewpoint the print is regarded, and so that the complex variation of the highlights we associate with viewing a 3D object occurs in front of our eyes.

In this work we propose and discuss a hybrid approach that combines 3D color laser scanning with 2D photography, using the camera images not as the source of the color in the final output, but as reference information for fine tuning color from the laser data.

The paper is organized as follows: first, we discuss 3D color imaging techniques and the color management issues arising from each. Next, we propose a hybrid color-managed process combining the respective strengths of laser scanning and 2D color photography. We then quantify color errors in 2D color imaging of 3D objects, and describe 3D laser image data processing. Finally we show how to eliminate high-error pixels from the reference image using geometric data from the laser scans.

3D Color Imaging

Color management raises important issues for 3D color imaging. Camera-based techniques include structured light projection with detection by two or more cameras, photogrammetry, and reflectance transformation imaging (RTI). The inherent strengths of camera-based techniques are the massive parallelism in simultaneous data acquisition, the broadband spectral response of the sensors, covering the visible spectrum, and the potential to achieve high resolution. The disadvantages relate to the presence in the resulting images of specular highlights, shadowing and shading (all of which are difficult to eliminate), challenges in absolute color calibration, controlling illumination across the field of view and geometric distortion in the collection lens. Specular highlights are particularly challenging with glossy artworks: Artusi et al. [3] reviewed approaches to eliminate specular reflection in 2D imaging. Rushmeier et al. [4] described elimination of specularity and shadows from color images during 3D structured-light scanning by using sets of images acquired with five light sources at different positions, turned on one by one. Such approaches are not widely practiced in structured light or photogrammetry. RTI is primarily a visualization methodology which enables re-lighting from any direction in order to facilitate interpretation of the appearance of physical objects. It can be used to estimate surface normals, and therefore could be employed to de-embed shading effects. It typically suffers from high long-range errors in the surface topography, and is not a true 3D imaging technique, only a means of creating the illusion of viewing a 3D object.

Another issue in camera-based imaging is absolute image calibration, which is important so that 3D reproductions match the lightness of the original object. Absolute calibration ensures, for example, that the reproduction of a pastel-colored flower in a painting by Van Gogh perfectly matches the original. It is conventional to use color targets such as the ColorChecker in photography. Although absolute calibration is usually not the goal, it is feasible with a color correction workflow more typically used in scanner calibration. However, a ColorChecker is a type of transfer calibration standard, normally measured with a spectrophotometer in the conventional unpolarized 45°/0° lighting/observation geometry. Use of such a target to calibrate photography is compromised to the extent that photographic conditions frequently differ from the standard configuration.

We turn now to color laser-based techniques such as those described by Blais et al [1]. The inherent strengths of such a system are the simultaneous determination of geometry and color, minimal

distortion, and the elimination of cast shadows. Also, the precise control and knowledge of lighting and detection directions for each point allow de-embedding of photometric effects due to surface orientation. The main drawback is metamerism due to the triple laser illumination, each channel of which is monochromatic. In the following we propose and discuss a method to overcome this issue.

Hybrid 3D Laser Imaging Process

From the preceding discussion it is apparent that no one 3D imaging technique can achieve results adequate for the very exacting requirements of reproducing the world's greatest art treasures. We therefore consider ways to combine two imaging modalities in a hybrid 3D process. While it is conceivable to combine two distinct 3D techniques, we have concentrated on the simpler approach of combining a 3D and a 2D technique.

2D studio photography is practised at a high level in every leading museum. We propose combining it with 3D polychromatic laser imaging. It is tempting simply to texture map a 2D image captured by calibrated photography to the 3D geometry captured by laser, but such an approach has several drawbacks. The first is the computational complexity and ambiguity in the registration and mapping process. More significant, however, is that 2D photographs of 3D objects are highly inaccurate in places. Even using multi-flash techniques to reduce (but never eliminate) specularity, the shadowing effects render direct use of the photographic images unsuitable, as we will show in the following section. On the other hand, 2D photography is a very good solution for color imaging of relatively flat surfaces. Our proposal is to use the 2D photograph as a reference image for the color, and to use the geometric information from the laser scans to select only pixels from the 2D image that are minimally affected by shading, cast shadows and specularity. We then employ the selected reference image pixels in color adjustment of the laser scan data, thereby overcoming the metamerism.

Photometric Errors in 2D Color Imaging

Shading

To quantify the impact of shading, consider the simplified plan of a studio setup in Fig. 1, where a flat object illuminated by two light sources (unit vectors $\vec{L}_1$ and $\vec{L}_2$) is imaged in direction $\vec{V}$ by a camera lens onto a linear detector pixel ds. The object has reflectance R $(0 \leq R \leq 1)$, and is oriented at surface angle θ; positive values of θ correspond to rotation around y as shown. We obtain the normalized reflectance by dividing by the signal from an ideal diffuse reference target with unity reflectance at $\theta = 0$:

$$\hat{I}(\theta) = R\,(I_1 \cos(\theta_1 - \theta) + I_2 \cos(\theta_2 - \theta))/(\cos(\theta_1) + \cos(\theta_2)) \quad (1)$$

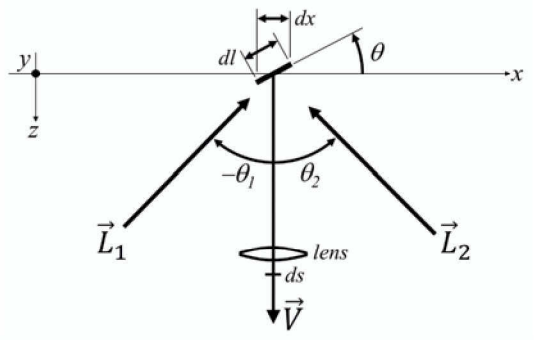

Figure 1: *Simple model of two light sources illuminating an object segment.*

We consider lights of equal intensity and an object with reflectance of 0.5, and show results as a function of surface angle in Fig. 2 (upper) for lighting at ±45°. Cusps are visible at ±45°, which occur when the surface becomes shadowed for one light. Similar behavior is seen for lighting at ±55° degrees and ±65° in the center and lower panels of Fig. 2, respectively. In this last case we see that with steeply raked lighting it is possible for the normalized reflectance to exceed the value when the same surface is flat. This last result is rather surprising; it is important to keep track of this potential during data processing as much color management will become problematic if camera raw values are "whiter than white."

We now calculate the color errors corresponding to these photometric results, which are wavelength independent and thus affect only the lightness L^*. By comparing to the "correct" value obtained when the surface angle is zero we calculate the lightness error, ΔL^* using the CIELAB formula. We show results for lighting at ±45°, ±55° and ±65° in the upper, center and lower panels of Fig. 3, respectively. It is apparent that unacceptable lightness errors are easily obtained for quite modest surface angles, so conventional photography of paintings with significant relief in the brushwork will usually show pronounced errors from shading. Surprisingly, using more raked light as shown in the lower panel of Fig. 3 can reduce the shading error for a given range of surface angles.

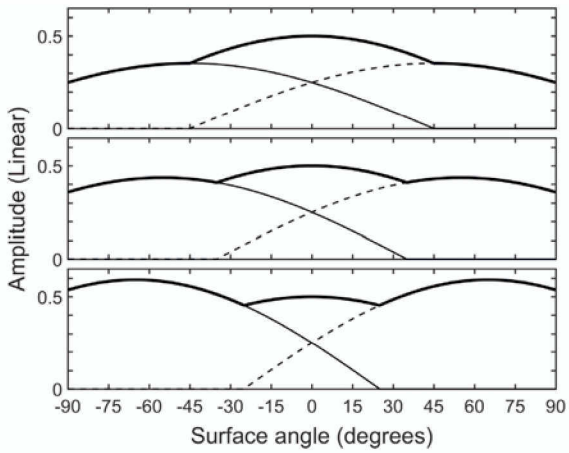

Figure 2: *Reflectance vs surface angle; illumination at: (upper) ±45°, (center) ±55° and (lower) ±65°. The light solid, dashed and heavy lines show results with source 1, source 2, and both sources, respectively.*

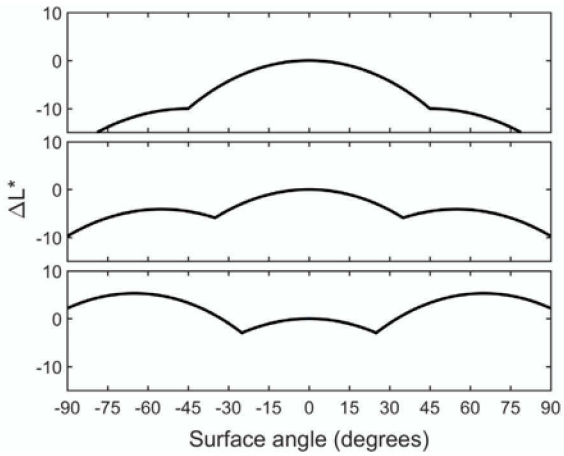

Figure 3: *Lightness errors vs surface angle, corresponding to Fig. 1: illumination at: (upper) ±45°, (center) ±55° and (lower) ±65°.*

Cast Shadows

The second deleterious effect in 2D imaging of 3D objects arises from cast shadows. While such effects may be obvious to the eye for isolated features, it is not widely recognized that shadows can play a significant role in creating errors in the fine structures that appear frequently in fine-art paintings. To illustrate how significant the effect can be, we printed a 3D test structure in a checkerboard pattern. All the squares are flat and uniform grey in color; half are displaced vertically with respect to the others by 0.5 mm; sidewalls are vertical. We imaged the structure in a perpendicular orientation using conventional high-resolution studio photography with two lights at ±45°. Results are shown in Fig. 4 for the sample, which contains five regions of varying dimensions of the individual squares as labelled. It is visually apparent that the decreasing dimension results in an apparent darkening due to the shadows; quantitatively the lightness difference is about $\Delta L^* = 5$.

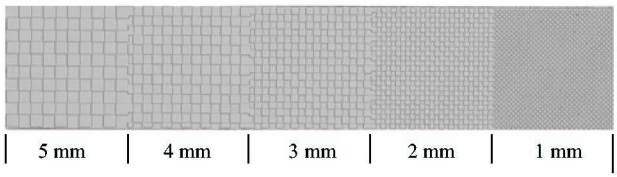

Figure 4: *Photographic image of checkerboard 3D test structure showing five regions with different square dimensions from 5 to 1 mm, as labelled.*

3D Color Laser Imaging

We perform laser imaging with a scanner design like that of Ref. [1], with single-mode lasers at 450, 532 and 638 nm focused and projected onto the sample surface with a scanning mirror. The wavelengths are close to the prime wavelengths identified by Thornton [5], except the red, which is about 30nm longer wavelength than the optimal. The reason for this is technological, and we have compromised somewhat on the wavelength to have the lower noise and complexity associated with a simple injection laser compared to a diode-pumped solid-state alternative.

Scattered light is collected via the rear surface of the same scanning mirror and raw color amplitudes detected for each color channel; a linear photodiode array is used to detect range. The line scanner is moved across the surface of the painting with a precision translation stage at two complementary angles, typically ±20°, relative to the painting normal. Color images and elevation maps with 254 dpi resolution (100μm pixels) are formed from point cloud data. Data from the two scans is registered and compared, with excessively light pixels rejected as specular. We perform calibration scans before and after painting scans using a series of flat Spectralon targets of varying reflectance factors to determine the black point and color channel gains. We also scale the raw color data for each point according to Lambert's law, with the surface normal determined from the geometric measurements, and the incident direction vector and distance from the detected point to aperture in the detection camera determined by instrument calibration. We have found this simple model very effective to de-embed photometric effects and yield excellent estimates of the object's reflectance at the three laser wavelengths.

Color Transformation

We have previously reported [6] a procedure for color transformation of the scanner image to match the corresponding colors in a reference photograph, both converted into the AdobeRGB color space. Here we explore the limitations of that approach and describe how they may be overcome. The procedure is illustrated in Fig. 5 by the painting *Jean-Pierre Hoschedé and Michel Monet on the Bank of the Epte* by Claude Monet (1890) in the National Gallery of Canada (Cat. 38089). The laser RGB signals are converted to CIEXYZ by a 3×3 matrix with coefficients derived from least-squares regression over 8,700 measured reflection spectra of real objects. The objective is to achieve an exact color reproduction [2], with identical chromaticity and absolute luminance at each point, so that the original and the print have the same colorimetric values when viewed side by side under the same illumination. The CIEXYZ values are then converted to Adobe1998 RGB; the resulting image is shown in the upper panel of Fig. 5. The reference image was corrected for geometric lens distortion and is shown in the lower panel of Fig. 5. An affine transformation is used to perform a global alignment of the reference image to the laser image, followed by resampling to 254 dpi and a spatially varying warping to achieve pixel-to-pixel alignment. Comparing the two panels of Fig. 5 it is apparent that the laser scanned image shows hue differences, especially in the green areas. It also lacks contrast because it was encoded with the black point intentionally raised to give enough dynamic range to account for thermal noise.

A color transformation was implemented by means of a lookup table (LUT), to convert each pixel of the laser scanned image to a

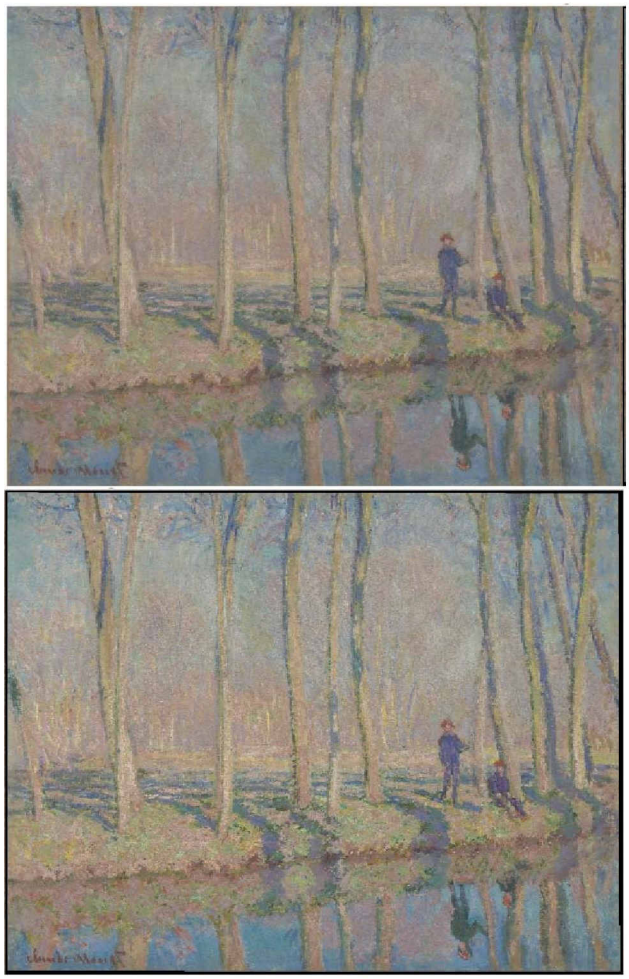

Figure 5: *Laser-scanned image (upper) vs photographic reference image (lower) of a painting by Claude Monet.*

color derived from the reference image [7]. In this case each 16-bit input RGB value is used to address the eight surrounding lattice values, and to perform a trilinear interpolation. The LUT is loaded from corresponding pixel values: the scanned RGB input value addresses the LUT and the reference image RGB value is the output. The resulting distribution within the LUT represents the distortion of color space applied to the image.

As noted in [6], the resulting adjusted scanned image was visually more accurate in hue, but darker than the reference image. Analysis of color differences indicated that in most places the errors were small, but that edges of image features showed larger errors resulting from self-shadowing of the surface relief by the oblique illumination from the photographic studio lights. This manifests as a large variance (scatter of values) of pixels in the photographic image associated with each RGB triplet from the laser image.

The reference image was photographed with studio lighting per Fig. 1 at ±45°. As discussed earlier, this leads to shading errors (Fig. 3, upper), and formation of cast shadows, where the side of a steep enough peak opposite the direction of the light source is obscured. The impact depends on the angle of the incident illumination, the local surface gradient, and the height of the brushstroke peak. Using the elevation data available from the 3D laser scanner as a digital elevation map (DEM), we can examine a 301×301-pixel detail of the Epte painting. The color data shows the head of the boy standing on the river bank (Fig. 6 upper left). The corresponding area of the DEM (Fig. 6 upper right), scaled so that white represents the highest points and black the lowest, shows a build-up of paint thickness over the forehead and hat brim and a convex profile across his chest. Gradients in the X and Y directions are calculated by taking differences along the respective X and Y axes (i.e. first-order partial derivatives). The X gradients are positive (light tones in Fig. 6 lower left) in local regions where the surface is rising to the right and negative (dark tones) where it is falling to the right. Similarly, the Y gradients (Fig. 6, lower right) are positive in regions where the surface is rising in the direction of increasing Y. The image contrast has been exaggerated to show the gradients more clearly. From the gradients the surface normal vector at each pixel is calculated.

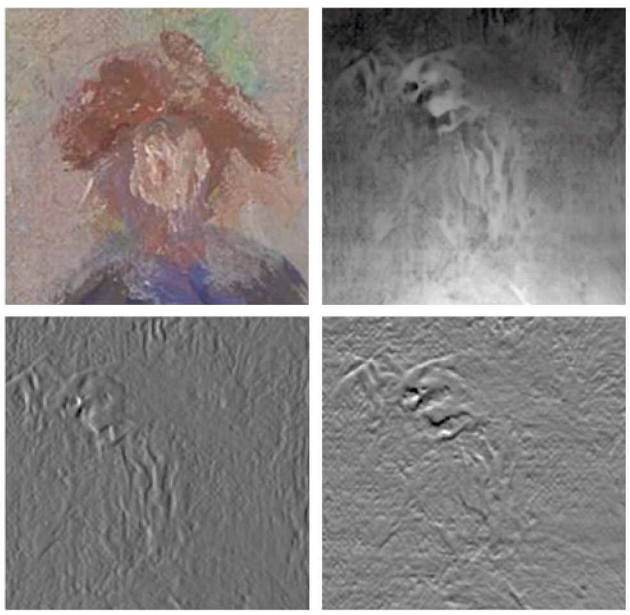

Figure 6: *(upper left) Detail of Epte painting; (upper right) elevation map; (lower left, right) X,Y gradients.*

Improved Color Transformation

The geometric data shown in Fig. 6 indicates how data used to build the LUT can include inaccurate color data from pixels in the reference image, which may result in significant errors in the final image. We use the geometric data available from the laser scanning to mask out pixels that are expected to exhibit high inaccuracy, ensuring that they do not contribute to the LUT values, and thereby improve the color transformation. In this section we describe how to do this geometrical filtering and show results for two paintings in the following section.

Avoiding Photometric Shading

The simplest mask to construct is for shading, using the surface normal data extracted from the elevation map. We exclude any point P for which the surface normal vector $\vec{N}$ is more than a specified angle $\alpha_{\max}$ from the view direction $\vec{V}$ (see Fig. 1), where shading errors are too great. Based on Fig. 3 we choose $\alpha_{\max} = 30°$. Effectively we are selecting pixels to build our LUT from regions that are close enough to the plane of the painting.

Avoiding 3D Cast Shadows

We use a simple algorithm for one-dimensional shadow casting, considering only the X component of the incident rays of light (Fig. 7, where the lighting angle sign convention is the same as Fig. 1). We form a shadow mask by proceeding from left to right, for each pixel if the surface gradient is more negative than the illumination gradient then the surface is in shadow, and the surface emerges from shadow only when its height exceeds the height of the downward ray. We consider illumination from left and right separately and combine the shadow masks.

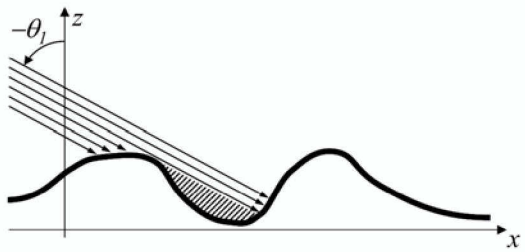

Figure 7: *A local peak casts a shadow on the side away from the direction of oblique illumination. The lighting angle sign convention is the same as Fig. 1.*

Avoiding Specular Highlights

As noted earlier, lighting a glossy 3D surface leads to specular highlights in the image, which may be reduced by multi-flash imaging. Alternatively, they may be eliminated using the geometric information from a laser scan as follows. Previous studies have shown that the intensity of the specular peak can be modelled effectively by the Lorentzian function centered on the specular peak angle [8]. The Lorentzian is superior to a Gaussian, being narrower in the peak and broader in the flanks, which fits better the distributions observed from typical materials. In practice, for color matching, angles within a cone of approximately $\beta_{\min} = 20°$ in radius about the specular peak need to be avoided because their reflectance is greater than the Lambertian body color. Fig. 8 shows the geometry at point P with unit vectors from the light source $\vec{L}$, surface normal $\vec{N}$, and view $\vec{V}$. The vector $\vec{H}$ lies halfway between $\vec{V}$ and $-\vec{L}$. If the surface normal $\vec{N}$ equals $\vec{H}$ the specular reflection of the incoming light is directed exactly in the view direction.

Around $\vec{H}$ is the perispecular zone, shown cross hatched, which is to be avoided, extending to $\beta_{\min}$ on either side of $\vec{H}$. For a given lighting vector the halfway vector can be calculated as:

$$\vec{H} = (\vec{V} - \vec{L})/2 \quad (2)$$

To ensure the surface normal vector $\vec{N}$ does not lie within the cross-hatched region proximity of $\vec{H}$, pixels are selected which satisfy:

$$\text{acos}(\vec{H} \cdot \vec{N}) > \beta_{min}. \quad (3)$$

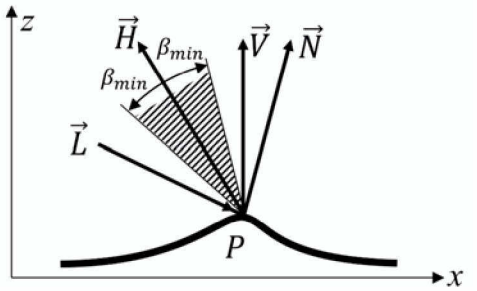

Figure 8: *Reflection geometry at a surface point. Specular highlights are avoided if the surface normal $\vec{N}$ lies outside the hatched region.*

Demonstration

In the preceding section we described ways to mask out pixels that are inaccurate from the reference image. Before showing results for specific paintings we first detail the process to build the LUT from the pixels remaining after masking. Over the course of applying this method to a variety of paintings we have found that several aspects of the LUT-creation process are important. First, before building the LUT it is beneficial to match the black and white points of the scanned image with those of the reference image. This is achieved by scaling each channel of the scanned image to match the corresponding channel of the reference image at 0.5 and 99.95 percentile points. Second, the number of cells in the LUT is chosen to have enough reference image pixels to fill the majority of the LUT cells from image data; we have found an average of at least 200 image points per cell yields good results and LUT sizes around 50×50×50; small paintings require correspondingly smaller LUT dimensions. Third, in populating the LUT we take the median of all corresponding values from the reference image; we will later examine the impact of this step in the Discussion section of the paper. Fourth, once the LUT is populated with all available data from the reference image, we fill any empty points within the image gamut using the median of non-empty nearest neighbors. Empty points outside the gamut play a limited role and are simply filled with the corresponding grayscale value. Finally, we perform a 3×3×3 median filter on all the LUT values.

We now turn to results of processing. While we motivated our work with a discussion of the Epte painting shown in Fig. 5, this work is quite matte and has subtle brushwork. To test the proposed method on a more challenging subject we turn to another painting, *Iris*, by Vincent van Gogh (1890) in the National Gallery of Canada (Cat. 6294). The laser-scanned image and reference photograph are shown in Fig. 9. This painting has a high level of gloss and flamboyant brushwork with an elevation difference of 8.82 mm across the painting. We will focus on a 300×450-pixel detail area around the flower in the upper-left-hand quadrant of the work; in Fig. 10 we show the corresponding laser-scanned and reference images, together with the elevation map scaled so that white represents the highest areas and black the lowest.

Figure 9: *Laser-scanned image (left) vs photographic reference image (right) of Iris by Van Gogh (1889).*

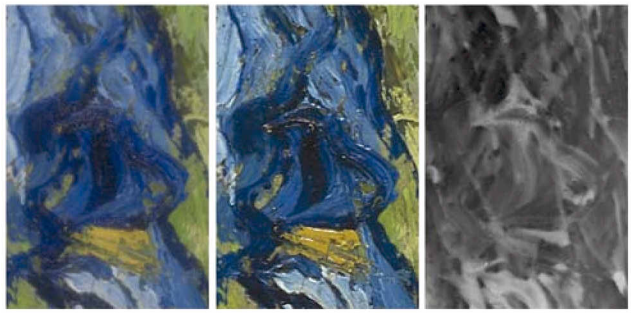

Figure 10: *Laser-scanned image (left) vs photographic reference image (center) and elevation map (right) of Iris in detail area.*

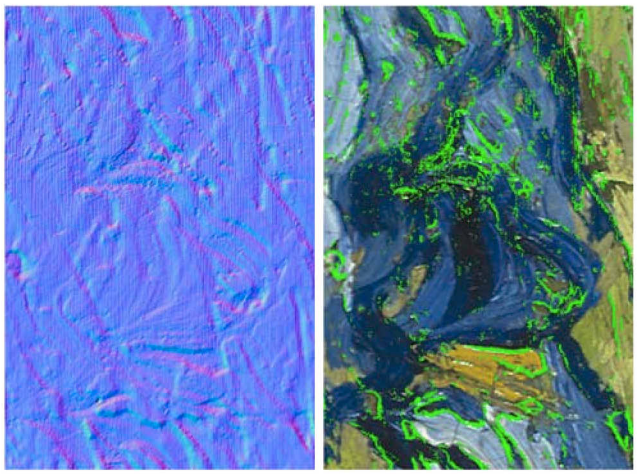

Figure 11: *Surface normal (left) and photometric mask (right) in green.*

In Fig. 11 we show the computed surface normals (left) and the reference image (right) with the pixels selected by the photometric shading mask shown in bright green. Using $\alpha_{\max} = 30°$ eliminates 9.6% of the pixels. In Fig. 12 we show cast shadows (left) for the lighting, which was at ±65° from normal (i.e. elevation of 25° from the plane of the painting). This eliminates 13.5% of the pixels. Finally, in Fig. 12 (right) we show the specularity mask with $\beta_{\min} = 20°$ as red pixels, which eliminates 10.9% of the pixels. Overall, the combination of all three geometric masks eliminates 23.4% of the pixels from inclusion in the LUT.

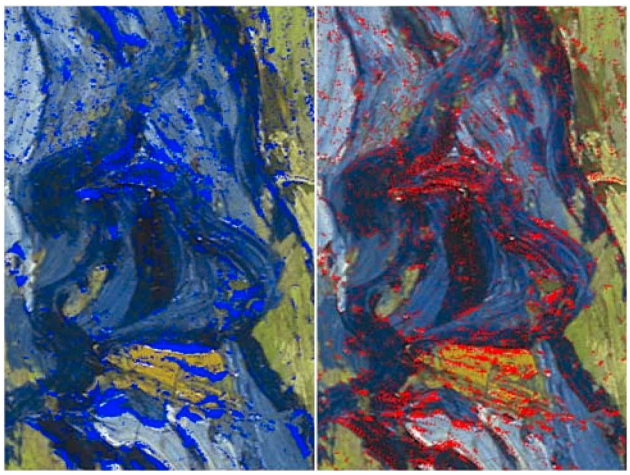

Figure 12: *Shadow mask (left) in bright blue; specularity mask (right) in red.*

Discussion

One of the challenges of this work is that we do not have access to any 3D "ground truth" about the painting color. Our careful examination of differences between the laser-scanned and reference images confirms that all three effects that contaminate reference photography are indeed present and are significant. It is therefore intuitive that eliminating them from the LUT should improve color accuracy in the final corrected laser-scanned image. To evaluate this hypothesis, we compare the corrected laser-scanned images with and without all geometric masks applied, i.e. using pixels from only the masked image or using the entire reference image. The resulting histogram of color differences is shown in Fig. 13, with a peak ΔE^*_{ab} of 0.33. Considering that this data is our best estimate of the degree of improvement attained using the geometric filtering we can see that the impact is rather modest – an average ΔE^*_{ab} of 0.49, with few values above 1.5.

Given that the masking process eliminated nearly 25% of the pixels in this detail area, this result is unexpected. We attribute it to the surprisingly good performance achieved by using a simple median filter to fill the LUT. While the data without any geometric filtering have significant variance, the median filter is effective at ignoring the outliers present in the reference image. By eliminating these outlier points using geometrically-based masks, we reduce the variance of the data from which the LUT is populated. However, the median of these less-scattered data in each LUT cell remains quite close to that of the full dataset.

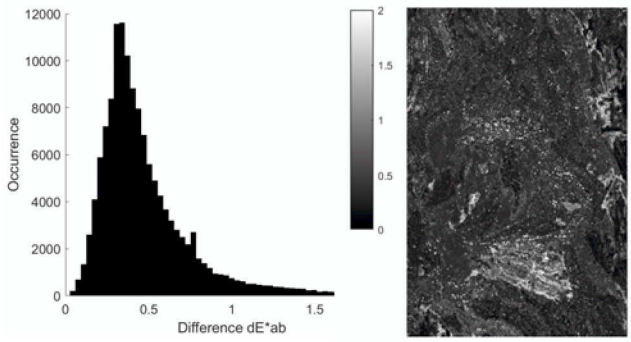

Figure 13: *Histogram and image of color differences between the corrected laser-scanned image including all geometric masks and no geometric masks.*

In the traditional graphic arts, reproductions are color matched using flat, matte uniform color patches. In 3D color reproduction, results depend on the interplay of illumination with the structure and gloss of the surface relief. The present work shows good 3D color management is achieved by combining two complementary techniques, polychromatic laser scanning and conventional photography. Future challenges lie in visual assessment of these complex 3D fine art reproductions compared to the originals.

Conclusion

We have proposed an empirical method of correcting metamerism in the color of a laser scanned 3D image using a photographic reference image. Shaded, shadowed and specular pixels can cause large color errors in the reference image, which can be eliminated by using geometric information from the laser scans to form masks. Surprisingly, results without masking are quite good due to the use of median filtering in the process. Therefore, use of the geometrical masking proposed in this paper is justified primarily to attain the highest possible quality in 3D fine art reproductions.

Acknowledgments

We thank L. Cook and C. Hupé of the National Gallery of Canada for painting photography, and K. Dyck for Fig. 4. This work has been supported by the National Research Council of Canada under the Industrial Research Assistance Program.

References

[1] F. Blais, J. Taylor, L. Cournoyer, et al. "Ultra High-Resolution 3D Laser Color Imaging of Paintings: the Mona Lisa by Leonardo da Vinci," in 7th Intl. Conf. on Lasers in the Conservation of Artworks, Madrid, 2007, pp. 435-440.

[2] R.W.G. Hunt, The Reproduction of Colour, 6th Ed., Chichester, John Wiley, 2004. pp.163-178.

[3] A. Artusi, F. Banterle and D. Chetverikov, "A Survey of Specularity Removal Methods," Computer Graphics Forum, Vol. 30, Issue 8, 2011, pp. 2208-2230.

[4] H. Rushmeier, G. Taubin and A. Guéziec, "Applying Shape from Lighting Variation to Bump Map Capture," in J. Dorsey, P. Slusallek (eds), Rendering Techniques '97, Springer, Vienna, 1997.

[5] W. A. Thornton, "Luminosity and Color-Rendering Capability of White Light," J. Opt. Soc. Am., Vol. 61, No. 9, 1971, pp. 1155-1163.

[6] L.W. MacDonald and M.K. Jackson, "Matching Reference Colours in 3D Reproduction of Fine-art Paintings," Proc. 13th AIC Congress, Jeju, Korea, 2017, OS19-5.

[7] L.W. MacDonald, "Color Laser Scanner Characterisation by Enhanced LUT," Proc. IS&T Conf. on Color in Graphics, Imaging, and Vision (CGIV), Amsterdam, 2012, pp.137-142.

[8] L.W. MacDonald, "Colour and Directionality in Surface Reflectance," Proc. Conf. on Artificial Intelligence and Simulation of Behaviour (AISB), Goldsmiths College, London, 2014. pp. 223-229.

Author Biographies

Mike Jackson received the B.Sc. in Electrical Engineering from the University of Alberta (1985) and the Ph.D. in Applied Physics from Caltech (1991). He is the Chief Technology Officer at Arius Technology Inc.

Lindsay MacDonald received his Ph.D. in image science from University College London (2015). He is a Fellow of IS&T, author of over 150 peer-reviewed articles and the co-editor of 10 books on colour imaging.